

Exploring the Noise Limits of Fully-Differential Micro-Watt Transimpedance Amplifiers for Sub-pA/ $\sqrt{\text{Hz}}$ Sensitivity

Ka-Meng Lei^{*}, Hadi Heidari^{†‡}, Pui-In Mak^{*}, Man-Kay Law^{*}, Franco Maloberti[†]

^{*}The State Key Laboratory of Analog and Mixed-Signal VLSI, University of Macau, Macao, China

[†]Department of Electrical, Computer, and Biomedical Engineering, University of Pavia, Italy

[‡]Electronics and Nanoscale Engineering Research Division, University of Glasgow, G128QQ, UK

yb27436@umac.mo, hadi.heidari@glasgow.ac.uk, pimak@umac.mo, mklaw@umac.mo, franco.maloberti@unipv.it

Abstract—This paper explores the noise performance limits of the differential configurations of differential transimpedance amplifiers (TIAs), which serve as a current detection front-end and converts signals for backend signal processing. TIA is one of the most frequent module adopted in biological and environmental sensing such as hall sensors and DNA synthesis detection, which require noise density down to sub-pA/ $\sqrt{\text{Hz}}$ with micro-watt power consumption so detailed analysis on the noise performance is required. The noises for three different TIAs, including the common-gate topology, op-amp based resistive feedback and capacitive feedback, have been investigated and simulated. Among them, op-amp based capacitive feedback, which bases on integration of input current, displays the lowest noise and best performance. Simulated in 180 nm CMOS process, the capacitive feedback technology shows an input-referred noise of 16 fA/ $\sqrt{\text{Hz}}$ (80 fA/ $\sqrt{\text{Hz}}$) at 10 kHz (100 Hz), featuring it a promising solution for current detection.

I. INTRODUCTION

The transimpedance amplifiers (TIA) are utilised to sense the current signals generated from the transducers (i.e., hall sensors and radiation detectors) and convert them into voltage readout with maximum signal-to-noise ratio for subsequent signal processing as most of the electronic modules such as analog-to-digital converters (ADC) are designed to co-operate with voltage signal. They are gaining increasing importance in the domain of single molecules and nano-scaled devices characterisation [1]. The resolution required in these applications is in the order of pA with bandwidth order in kHz, which turns out low-noise (< hundreds fA) electronic front-end with moderate bandwidth (<10 kHz) is entailed to convert the current signals to voltage signals [2]. For practical reasons, low current detection can be conducted with capacitors or resistors as passive sensing elements [3], [4] and [5].

A general model of the transducers together with the TIA and back-end electronics is shown in Fig. 1. The transducer detects the variation of the target (e.g., magnetic field for hall sensor or target DNA for nanopore) and produces a current output to the TIA. The TIA detects the diminutive current signals and transduces them into corresponding voltage signals. The back-end signal processor may include buffer or filter to drive the subsequent ADC before digitising. This paper focuses on the analysis of the TIAs and provides extensive

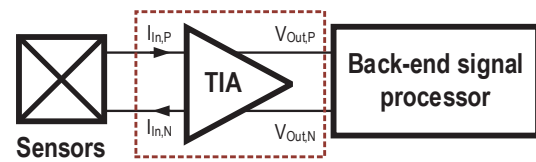


Fig. 1. The block diagram of the sensor, analog front end (TIA) and back-end signal processor.

studies on the TIAs for their transfer characteristics and noise performance in order to implement a low-power low-noise TIA for current sensing application. Three different kinds of TIAs have been analysed and compared: the pseudo-differential common-gate topology, fully differential resistive feedback type TIA and capacitive feedback type TIA.

The paper is organised as follows: in the next Section, the transfer functions and noises of current-to-voltage transimpedance amplifiers are derived and a performance comparison is discussed. Section III shows the simulations in different topologies of the differential TIAs. Section IV draws the conclusion of the paper.

II. DIFFERENTIAL TRANSIMPEDANCE AMPLIFIERS

In integrated CMOS technology, there are three ways of current sensing techniques: pseudo-differential common-gate topology, fully differential resistive feedback type TIA and capacitive feedback type TIA based on operational amplifier.

The first one is the common-gate topology, as shown in Fig. 2(a). The differential output current of sensor, $I_{In,N}$ and $I_{In,P}$, flows into the sources of a common-gate stage (N-channel input). The transresistance gain of the common-gate topology can be derived as $2R_D$. As it does not involve any feedback (both differential and common-mode), this makes it an easier approach to transduce the current input to voltage output. However, the transresistance gain of this topology is limited by the voltage drop across the resistor R_D . To maintain a reasonable output common level at a constant bias current, its transresistance is limited and a wide tuning range of the transresistance is unfeasible. Additionally, the transistor M_1

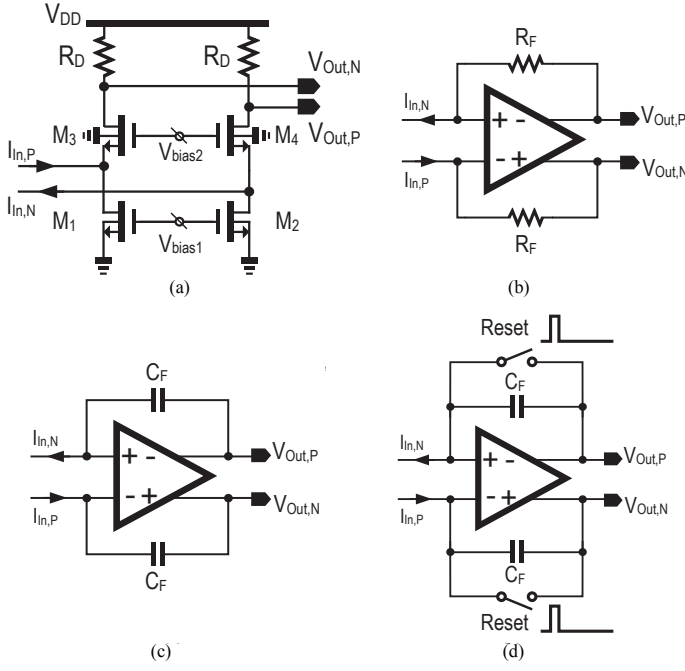


Fig. 2. Schematic diagram of (a) Pseudo-differential common-gate topology, (b) Resistive feedback type TIA, (c) Capacitive feedback type TIA and (d) Capacitive feedback type TIA with resetting switch.

(M_2) will contribute significant thermal noises directly to the output of the TIA. The input-referred noise can be derived as:

$$\overline{i_n^2} = \frac{2kT}{R_D} + \frac{\overline{i_{n,M1}^2}}{2} \quad (1)$$

where k is the Boltzmann constant, T is the temperature in Kelvin and $\overline{i_{n,M1}^2}$ is the noise current spectral of the bias transistors M_1 (M_2) and assuming an infinite output resistances of the transistors. One main drawback for this topology is that it is pseudo-differential, which means the common mode noise from the input will directly couple to the output. This increases the burden on the CMRR of the subsequent stage thus it is rarely used in low-noise application.

The second topology is the resistive feedback type TIA as shown in Fig. 2(b). It is in fully-differential configuration so all the common-mode noise from the sensor can be rejected at the output, rendering it favourable for low-noise application. The output current of the sensor is sensed by the resistor R_F . By applying Kirchhoff's circuit laws at the input pairs of the TIA, the output voltage expression for the resistive feedback type TIA can be expressed as (assuming ideal op-amp):

$$V_{out} = V_{out,P} - V_{out,N} = 2R_F I_{In} \quad (2)$$

The noises generate in the resistive feedback type TIA can be divided into two components: the thermal noise from the resistor and the input-referred noise of the op-amp $\overline{V_{n-op}^2}$. The output-referred noise voltage at low frequency (i.e., at the frequency band of interest) could be shown as:

$$\overline{V_{n,out}^2} = 8kTR_F + \overline{V_{n-op}^2} (1 + j\omega R_F C_{in})^2 \quad (3)$$

where C_{in} is the input capacitance of the op-amp (each terminal). The input-referred noise of the op-amp is the sum of two components, namely the flicker noise $\overline{V_{n-op,flicker}^2}$ which noise spectral density is inversely proportional to the frequency and the thermal noise $\overline{V_{n-op,thermal}^2}$ which is independent of frequency. The input-referred noise current for the TIA is the output-referred noise voltage divided by the transresistance gain of the TIA:

$$\overline{i_n^2} = \frac{2kT}{R_F} + \frac{\overline{V_{n-op}^2} (1 + j\omega R_F C_{in})^2}{4R_F^2} \quad (4)$$

It can be observed from eq. (4) that to reduce the input referred noise of the TIA, the value of the transresistance R_F should be increased. Yet this will increase the area and instability of the TIA, causing a trade-off on the performance on the TIA.

The third method is capacitive detection as shown in Fig. 2(c). Similar to the resistive feedback type TIA, this configuration is also in fully-differential so all the common-mode noise can be rejected at the output. The currents $I_{In,N}$ and $I_{In,P}$ are integrated over the capacitor C_F . However, any baseline drift and offsets of the sensors and amplifiers will saturate the output of the op-amp and disturb the operation of the TIA. To resolve the issue, reset switches are added parallel to the capacitors, as shown in Fig. 2(d). The voltage across the capacitors now will reset at a fixed interval thus the saturation problem of the op-amp can be eliminated.

The transfer function of the capacitive feedback type TIA is not as straight forward as resistive feedback type since it involves reset switches in the circuit. At the reset phase, both of the outputs are discharged to output common mode voltage V_{CM} , producing a zero output at this phase. After the reset phase, the TIA enters the integration phase and the input current will charge the feedback capacitors with the input currents. The voltages across the feedback capacitors at the end of the integration time T can be expressed as:

$$V_C = -\frac{1}{C_F} \int_{t_{start}}^{t_{start}+T} I_{In}(t) dt \quad (5)$$

assuming the voltages across the capacitors have been discharged to zero at the end of the reset phase and t_{start} is the starting time of integration. Thus the output voltage of the TIA at the end of the integration is two times the voltage across the feedback capacitor:

$$V_{out} = V_{out,p} - V_{out,N} = \frac{2}{C_F} \int_{t_{start}}^{t_{start}+T} I_{In}(t) dt \quad (6)$$

Considering a sinusoidal current with amplitude i_A and angular frequency ω is applied to the capacitive feedback type TIA, the output of the TIA will become:

$$V_{out} = \frac{2}{C_F} \int_{t_{start}}^{t_{start}+T} i_A \sin \omega t dt \quad (7)$$

$$V_{out} = \frac{2i_A}{C_F} \left\{ \frac{1}{\omega} [\cos \omega(t_{start})] - [\cos \omega(t_{start} + T)] \right\} \quad (8)$$

If the input frequency is much smaller than the sampling frequency, after simplification can be obtained:

$$V_{out} = \frac{2T}{C_F} * i_A \sin \omega t_{start} * \frac{\sin \frac{\omega T}{2}}{\frac{\omega T}{2}} \quad (9)$$

which shows a DC transresistance gain of $\frac{2T}{C_F}$ at low frequency as the last term ($\sin(\frac{\omega T}{2})/\frac{\omega T}{2}$) will approach zero and the gain can be altered by the capacitor feedback C_F . At frequency comparable or higher than the sampling frequency, the output of the TIA forms a low-pass filter which can filter the high frequency noise of the input sensor.

The output-referred noise voltage of the capacitive feedback type TIA can be expressed as:

$$\overline{V_{n,out}^2} = \overline{V_{n-op}^2} (1 + \frac{C_{IN}}{C_F})^2 \quad (10)$$

and the input-referred noise current of the capacitive feedback type TIA can be obtained as the output-referred noise voltage divided by the transresistance gain of the TIA:

$$\overline{i_n^2} = \overline{V_{n,out}^2} (\frac{C_F}{2T})^2 = \overline{V_{n-op}^2} (\frac{C_F}{2T} + \frac{C_{IN}}{2T})^2 \quad (11)$$

It can be observed that to minimise the input-referred noise current of the TIA, the transresistance gain of the TIA should be increased while the input capacitance of the op-amp should be decreased. Different from the resistive feedback type TIA, an increase in transresistance of the capacitive type TIA entails a lower capacitance for the feedback capacitor (i.e., smaller die size), rendering it favourable for low-noise application.

III. SIMULATION RESULTS

Simulations are performed in conventional CMOS 180 nm process. The telescopic op-amp with supply voltage of 1.8 V is employed. The dc gain of the op-amp is 84.3 dB and GBW is 2.22 MHz with bias current of 1.2 μ A. The phase margin is 88° with load capacitors of 1 pF. Fig. 3 shows the open-loop input-referred noise density of the op-amp for reference.

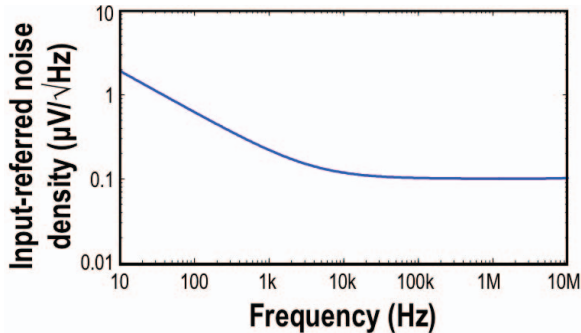


Fig. 3. Open-loop input-referred noise density of the op-amp.

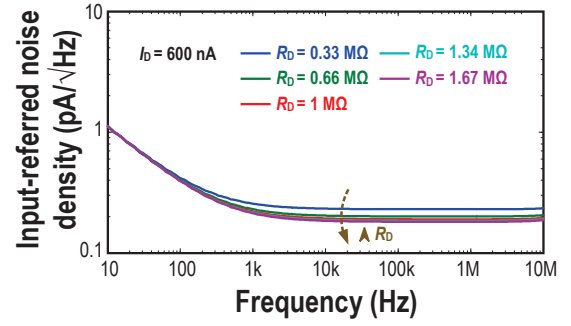


Fig. 4. Input-referred noise of the common-gate TIA with varying R_D .

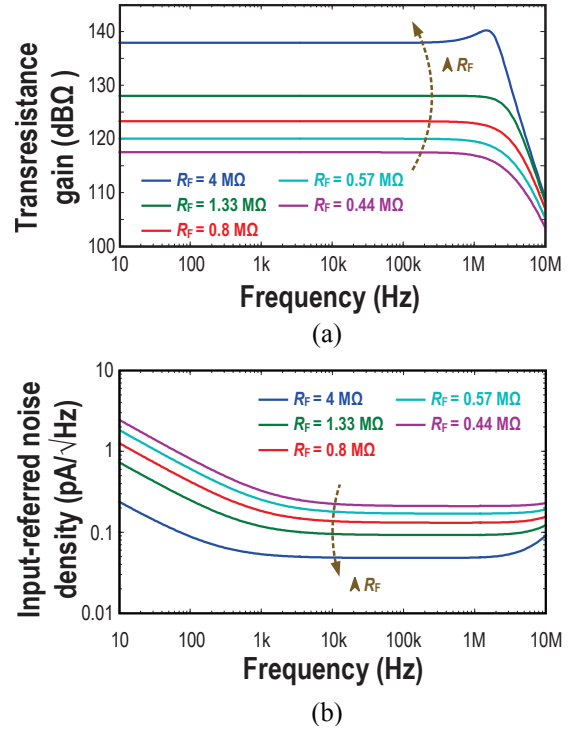


Fig. 5. (a) Transimpedance gain of the resistive feedback type TIA of different feedback resistance R_F , (b) Input-referred noise of the resistive feedback type TIA with varying R_F .

the bias transistors are directly added to the overall noises attributed to the non-feedback structure of the common-gate topology so this topology shows a an input-referred noise of 180fA/√Hz (390fA/√Hz) at 10 kHz (100 Hz) and R_D of 1.67 MΩ). For low-noise and low-power application this topology is not preferable compared to the op-amp base approaches.

Transresistance gain of the resistive feedback type TIA of different feedback resistance is shown in Fig. 5(a). The gain increases linearly with the resistance of R_F . However, at R_F of 4 MΩ, there is an overshoot for the transresistance gain at around 1 MHz, which indicating the instability of the TIA thus the tuning range of the transresistance gain for the TIA is confined. The simulated input-referred noise of the resistive feedback type TIA is shown in Fig. 5(b). It can be

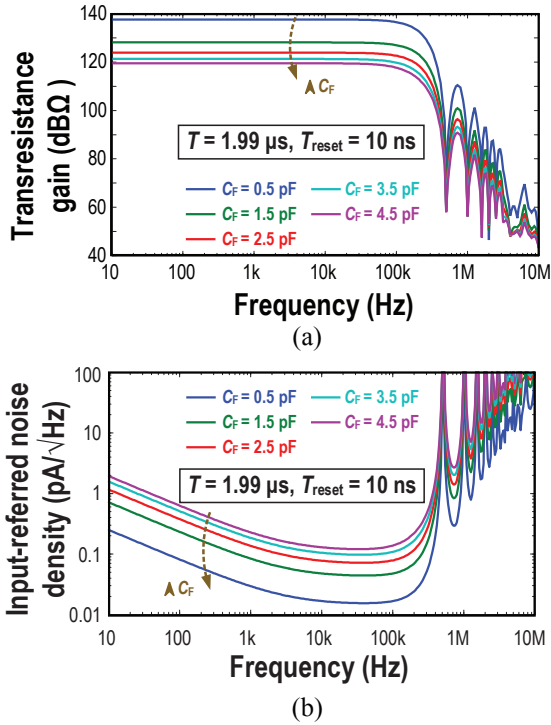


Fig. 6. (a) Transimpedance gain of the capacitive feedback type TIA of different feedback resistance C_F , (b) Input-referred noise of the capacitive feedback type TIA with varying C_F .

noted that the input-referred noise current is decreasing with a higher feedback resistance (transresistance gain) as described in eq. (4). The input-referred noise at a gain of 138 dB and frequency of 10 kHz (100 Hz) is 50 fA/√Hz (89 fA/√Hz), which is significantly lower than the common-gate topology even with similar power consumption.

The transresistance gain and input-referred noise of the capacitive feedback type TIA with different values of feedback capacitance are shown in Fig. 6(a) and (b), respectively. The transresistance gain of the TIA increases with a decreasing feedback capacitor in a fixed integration time of 1.99 μs (sampling interval of 2 μs), which is matched with eq. (11). Furthermore, there is a sharp roll-off at frequency larger than sampling frequency (500 kHz), attributed to the low-pass characteristics of the capacitive feedback and the frequency response of the op-amp. On the other hand, the input-referred noise decreases together with the feedback capacitor exhibiting a noise current density of 16 fA/√Hz (80 fA/√Hz) at 10 kHz (100 Hz) and a gain of 138 dB, which is lower than the resistive counterpart since the feedback network does not introduce thermal noise. This property implies tantalizing advantage and renders it a promising solution for low-noise biomedical application where the bandwidth of the signal is limited (usually <100 kHz).

Interestingly, at low frequency where the flicker noise of the op-amp dominates the input-referred noise of the TIA (i.e., $V_{n-op,flicker}^2 \gg 8kTR_F$), the capacitive feedback type TIA exhibits a higher input-referred noise than the resistive

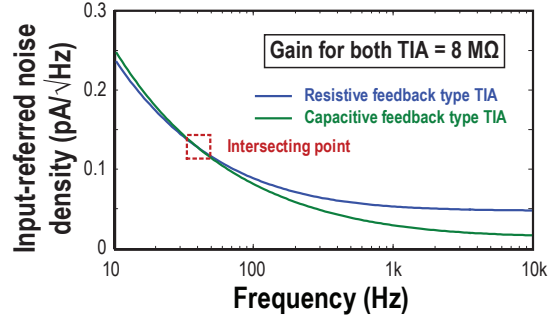


Fig. 7. Comparison of the input-referred noise of the capacitive feedback and resistive feedback type TIAs.

counterpart since its performance will be deteriorated by the input capacitance of the op-amp C_{in} , a phenomenon which is not observed in the resistive feedback type TIA. As verified in Fig. 7, the resistive feedback type TIA has a better input-referred noise at frequency below 40 Hz. Yet, for moderate frequency where thermal noise of the feedback resistor is comparable or larger than the input-referred noise of the op-amp, the capacitive feedback type TIA still demonstrates a better noise performance.

IV. CONCLUSION

This paper presents a comprehensive analysis on low-noise current detection readout systems and compares the performance of different types of differential transimpedance amplifiers for biomedical and environmental applications. Simulations are performed in a standard 180 nm CMOS technology. Based on theoretical analysis and simulation results, the capacitive feedback type TIA with reset switches displays the best noise performance of 16 fA/√Hz (80 fA/√Hz) at frequency around 10 kHz (100 Hz), which makes it suitable for low-noise and high resolution applications.

ACKNOWLEDGMENT

This work was supported by the Research Committee of the University of Macau Science and Technology Development Fund - FDCT (047/2014/A1).

REFERENCES

- [1] G. Ferrari, F. Gozzini, A. Molari, and M. Sampietro, "Transimpedance amplifier for high sensitivity current measurements on nanodevices," *Solid-State Circuits, IEEE J. of*, vol. 44, no. 5, pp. 1609–1616, 2009.
- [2] M. Crescentini, M. Bennati, M. Carminati, and M. Tartagni, "Noise limits of cmos current interfaces for biosensors: A review," *Biomedical Circuits and Systems, IEEE Transaction on*, vol. 8, no. 2, pp. 278–292, 2014.
- [3] D. Kim, B. Goldstein, W. Tang, F. J. Sigworth, and E. Culurciello, "Noise analysis and performance comparison of low current measurement systems for biomedical applications," *Biomedical Circuits and Systems, IEEE Transaction on*, vol. 7, no. 1, pp. 52–62, 2013.
- [4] H. Heidari, E. Bonizzoni, U. Gatti, and F. Maloberti, "A 0.18-μm cmos current-mode hall magnetic sensor with very low bias current and high sensitive front-end," in *Sensors, 2014 IEEE*, Nov 2014, pp. 1467–1470.
- [5] Y. Tang, Y. Zhang, G. Fedder, and L. Carley, "An ultra-low noise switched capacitor transimpedance amplifier for parallel scanning tunneling microscopy," in *Sensors, 2012 IEEE*, Oct 2012, pp 1–4.